Research on Engineering Structures & Materials
www.jresm.org
MIM Research Group

Research Article

Experimental and computational investigation of stiffened composite panels with compression after impact

Aleksandr Bolshikh[*,a], Marina Klesareva[b], Egor Nazarov[c], Bogdan Ustinov[d]

Moscow Aviation Institute (National Research University), Moscow, 125993, Russia

Article Info

Article history:

Received 31 July 2024
Accepted 23 Nov 2024

Keywords:

Finite element methods;
Low-speed impact;
Load-bearing capacity;
Delamination,
Barely visible impact damage

Abstract

In this paper the load-bearing capacity of a stiffened stringer panel made of polymer composite materials (PCM) reinforced by intermediate modulus carbon fiber under compression after impact was investigated. Computational-experimental investigations were conducted to assess obtained results where stringer panel was loaded to failure. In this paper, a computational and experimental method for modeling the compression after Impact and failure mode for single-span composite panels with barely visible impact damage (BVID) is proposed based on the building block approach. The above-mentioned approach implies step-by-step test series coupled with simulations which are carried out on each stage gradually introducing larger and structurally more sophisticated test samples. That approach serves as the base for design of composite structures by means of increasing the number of smaller test samples and carrying out a lot of simulations in order to reduce the margin of error and to reduce the number of large test structures (wing, fuselage, etc.) required for proof of compliance of the proposed airframe to available design objectives thus cutting the cost of experimental program. Further the model of material behavior was developed considering combined loading caused by growth of cracks and delaminations. For that material model a series of coupon tests were performed to refine elastic and strength parameters of material. Consequently, a ply-by-ply solid finite element model (FEM) of the stiffened two-stringer panel with cohesive interface behavior was developed. Test samples of the stiffened panels made by vacuum resin infusion were subjected to impact damage between the stringers followed by compression in the testing machine with two edges fixed as cantilever beams. Robustness of the proposed simulation method and suggested modelling approach was confirmed by similarity of obtained numerical results and experimental data as well as the similarities of the failure mode and state upon failure.

1. Introduction

Today, it is probably impossible to name the areas of technical systems where composite structures are not used. Aircraft manufacturing is considered to be the leading industry employing load-bearing structures made of polymer composite materials (PCM). A large number of research programs are carried out all over the world to implement new composite technologies in various types of structures and new methods of analysis of strength under different loading modes [1-3]. In recent years, a number of articles containing strength criteria and various modelling techniques using numerical simulation of composite materials have been published [4-5]. Damage tolerance of aircraft stiffened composite panels has recently been a major concern.

[*]Corresponding author: bolshikhaa@mai.ru
[a]orcid.org/0000-0002-6740-3870; [b]orcid.org/0009-0005-4341-964X; [c]orcid.org/0000-0002-8614-9126; [d]orcid.org/0009-0002-3685-7682
DOI: http://dx.doi.org/10.17515/resm2024.372cs0623rs

Numerical modelling is a powerful tool to better understand the mechanics of complex multilayer composite structures. Previous works related to numerical and experimental studies of behaviour of composite structures with impact damage, delamination failures and damage tolerance were presented in [6-7]. Improving the efficiency of such structures requires a deep understanding of the types and principles of their operation, the use of a comprehensive approach, as well as multidisciplinary research. The experimental and numerical approach presented in [8] is applicable to all industries: helicopter, marine, automotive and many other areas are all employing experimental and numerical building block approach, sometimes referred to as "certify by analysis".

The contribution of the authors of this work to the development of the above-mentioned approach consists, among other things, in introduction of the principles of creating universal numerical models applicable for simulation of static, dynamic and fatigue strength of composite structures at different stages of design. The assessment of the residual strength of the reinforced composite panel during operation, presented in this work, is an integral part of the comprehensive work on the justification of the durability of the structure, considering potential manufacturing defects (delaminations), in-service damage of the four main categories, restoration of strength through local repairs and maintaining the load-bearing capacity of the structure at the ultimate load level until the design service goal [9]. The resistance to impact damage remains an important issue in the design damage tolerant structures found in fuselage compartments, wing boxes, tail planes, etc. Impact damage, which is mainly characterized by matrix cracking, delamination and fiber breakage, usually extends far beyond the point of impact. Such damage [10] is mainly present inside the laminate and is difficult to detect visually from the outside. Even in the case of a low velocity/low energy impact, the residual compressive strength can be significantly reduced.

To study the compressive load-bearing capacity of double-stringer reinforced panels with impact damage in the interstringer zone, a review of modern works on the considered subject [11-15] was conducted and a list of structural-like single-span flat panels, representing a rectangular plate (skin) reinforced in the longitudinal direction by two stringers, was formed. The thickness and width of the skin are variable parameters in the problem under consideration. At the first step, an impact with energy of 140 J, 103 ft-lb was simulated to represent a maintenance toolbox dropped on the skin surface [16]. Absolutely rigid clamps on all edges of the panel were defined by boundary conditions according to ASTM D7136 [17]. Post-impact compression was implemented by creating rigid plates simulating the base and traverse of the testing machine. The motion of the traverse of the testing machine was defined via boundary conditions in the form of displacement along the longitudinal axis, while the remaining degrees of freedom were fixed.

The panel was supposed to fail along the cross section weakened by impact damage accompanied by disbonding between the skin and stringers. The results of simulations based on the presented FE model in accordance with the building block approach [8] should allow to refine the material allowable normally established at the conceptual design stage in order to prove compliance to the requirements of articles CS-25.571 and CS-25.631 during certification [9]. In accordance with the requirements of the Advisory Circular [18] to the article CS-25.571 [9], the design of airframe primary structures made of PCM must ensure an appropriate load-bearing capacity for each of the four categories of in-service damage. According to that article, the design must meet: 1) environmental effects (including specified design parameters and impact damage); 2) static strength (including repetitive loads, tests of environmental effects, manufacturing process, dispersion of properties and impact strength); 3) evaluation of fatigue strength and allowable damage; 4) others - flutter, repairability, maintainability, etc. Compliance with

these requirements and competitive level of weight perfection of modern construction made of PCM is achieved by selection of design parameters for optimal joint operation of shells and stringers as well as by using the highest design characteristics of the material and by allowing for manufacturing defects of certain size and impact damage of certain energy values.

Building block approach followed by this study for the composites analysis is similar to unit cell concepts periodic structures (only one unit cell is used for analysis to get results for whole structure) finite element free vibration and flutter analysis applied to periodic line supported plate and shell as in [19-20] and some review studies that related to static, free vibration and buckling analysis of composite beam, plate and shell panels [21].

This topic has been extensively studied by simulating low-velocity impact with different energy values [22-25], modelling residual strength, combined fracture modes on the example of thin panels [26-31]. Approaches to solving the problems vary. A modern method can be considered "layer-by-layer modelling", which gives a sufficiently high accuracy and allows taking into account the properties of each layer with initialization of the fracture criterion. This allows getting the most complete picture of delamination not only of the entire panel, but also of an individually selected layer.

Most of the publications focus on simulating impact on thin-walled panels. However, when dealing with thicker laminates, additional problems arise. In particular, local compressive stresses significantly affect the initiation and propagation of interlayer damage and the occurrence of cross plane effects (interlayer shear and normal stresses). In addition, impact can cause damage that can locally divide the package into several sub-packages. Such damage may lead to local buckling under compression or shear action, redistributing critically these loads and causing both in-plane and out-of-plane stress concentrations. While undoubtedly most structures are made of thin laminates, in some aerospace and automotive applications the laminate is several centimetres thick. For long-haul aircraft, this can be in excess of 20-30 mm. This paper proposes a methodology for numerical "layer-by-layer modelling" of a large-thickness panel, considering an extended formulation of the model of cohesive interlayer interaction. The results of calculations according to the proposed method are in satisfactory agreement with the test results.

2. Research Methods

2.1 Tests

In accordance with the experimental and numerical building block approach, the proof of airframe primary structures is mainly performed by PCM coupon and structure-like specimen tests with various in-service damages. The purpose of such tests is to determine the residual safety factor, to confirm the design stresses and deformations accepted at the design stage, and to study the failure mechanism. Structural-like specimens are normally a set of structural elements, the tests of which allow estimating the strength characteristics of a full-scale structure without any recalculations and additional analysis.

In this work, experimental studies of the compressive strength of double stringer wing panels after an impact damage with an energy of 140 J in the interstringer zone and further determination of the load-bearing capacity of a typical section of the wing boxes skin under compressive load were carried out. The impact energy of a pile driver with an energy of 140 J was chosen to inflict BVID type impact damage in double stringer wing panel in the interstringer zone.

BVID includes acceptable defects and damage that may remain undetected during routine inspections. Tolerance of damage in this category requires demonstration of static strength under design loads throughout the service life of the aircraft. Such damage

includes defects and damage that occur during both manufacturing and service, such as minor delaminations, porosity, minor scratches, and minor environmental damage. The object of tests is single-span double-stringer flat panels made from carbon tape and epoxy resin by vacuum infusion method. The overall dimensions of the panel are presented in Table 1.

Table 1. Panel dimensions

Length, mm	Width, mm	Skin thickness, mm
350	231	10.8

The panel edges are reinforced with fiberglass overlays to prevent fracture where forces are applied Fig. 1. General view of Double-stringer panel on the test bench before and after fracture illustrated in Fig. 1. and Fig. 2.

Fig. 1. Double-stringer panel on the test bench before fracture

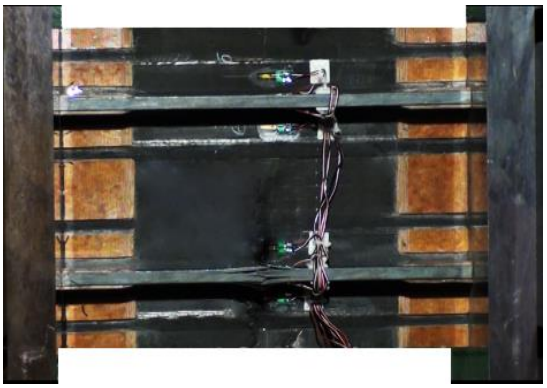

Fig. 2. Double-stringer panel on the test bench after fracture

A carbon bundle was placed between the stringers and the cladding. This test requires that the center of gravity of the panel cross section coincide with the line of action of the compressive forces of the testing machine. The stiffness of the test machine supports must be sufficient to ensure uniform distribution of compressive forces, which were monitored by means of strain gauges mounted on the panels. The panels were loaded until their bearing capacity was exhausted, and the following parameters were recorded: velocity of the impactor, force in the contact zone, compression force, displacement in the middle

section of the panel on the skin and on the stringer walls. The panels with a nominal thickness of 10.8 mm of cladding were destroyed in a section weakened by impact damage, with delamination of the cladding and stringers material. The defect area was 49x52 mm, the critical load was 1630 kN.

2.2 Computational Model

2.2.1. Geometry and boundary conditions

The finite element model consists of several parts: skin, L-shaped part of stringer, filler and impactor. The dimensions of the panel are shown in Table 1. The general view of the panel is shown in Fig. 3.

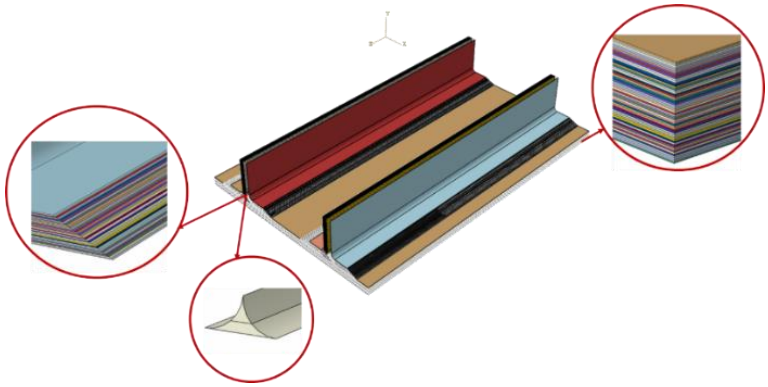

Fig. 3. General view of the panel

The impactor was modeled as a solid body with a mass of 5.5 kg. It has a spherical impact surface with a diameter of 25 mm and a height of 22.5 mm. The velocity of the impactor has only a vertical component equal to 7067 mm/s and is set by means of the initial velocity. At the same time, the initial velocity of the impactor was set using a special function of the Abaqus software - Predefined field, Initial velocity. The impact supports are not modeled in this calculation. We assume that this jig is absolutely rigid and contacts the panel in such a way that it is possible to accept a completely rigid termination (clamped tip) as boundary conditions on all sides of the panel according to ASTM D7136 [20], that is, clamping on all components of displacement and rotation.

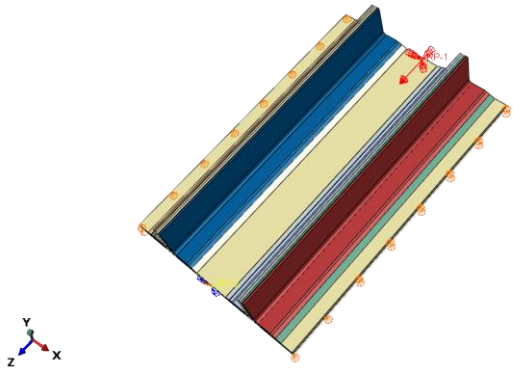

Fig. 4. Boundary conditions for compression after impact

The simulation of compression after impact was implemented as follows: 1) the test machine was simplistically modeled using absolutely rigid plates, that is, one of the plates was responsible for the base of the test machine and absolutely rigid boundary conditions were applied to it, the second plate was responsible for the movable crosshead of the test machine, to which boundary conditions were applied as longitudinal motion; 2) a reinforced double stringer panel was placed between the two plates; 3) inter-surface contacts were specified between the plates and the panel, and an additional gap was specified between the panel and both plates to avoid penetration of the surfaces into each other. In addition, additional boundary conditions were applied at the free edges to avoid loss of stability of the free edges of the cladding (anti-buckling supports), and thus preventing critical stress redistribution from occurring, allowing the weakened section to be incorporated after impact (Fig. 4.).

2.2.2 Description of The Finite Element Model

To investigate the compressive load-carrying capacity of a double stringer flat panel with impact damage in the interstringer zone, a layer-by-layer solid rectangular plate (cladding) supported in the longitudinal direction by two stringers was modeled. The stacking scheme is shown in Table 2.

Table 2. Layout

	Number of layers	Monolayer thickness	Packages Stacking
Skin	60	0.18	+45/0/-45/0/90/0/-45/0/+45
Stringer	29	0.18	+45/0/-45/0/90/0/-45/0/+45

A 0-degree layer is placed between the neighboring packages consisting of 9 layers. The calculation of the finite-element model is performed in two steps in the Abaqus software package - Dynamic Explicit:

- The first step simulates the impact
- The second step simulates the compression after the impact

The impactor is assigned with an initial velocity in the vertical direction. Its value should not be more than 1 percent of the speed of sound propagation in the medium (material):

$$\upsilon \leq 0.01 \cdot a \tag{1}$$

Where υ - initial velocity in the vertical direction, a - speed of sound propagation in the medium (material). This relationship was obtained after a series of computational tests to eliminate unrealistic local element stresses and inertial effects that cause increased initial strain resistance. Observing the condition (1), the value of kinetic energy equal to 140 J is selected. Residual strength is determined by the value of the reaction force occurring in the termination (plate).

All parts were modeled as solid with C3D8 mesh elements Fig. 5 using full integration to avoid additional element distortion (hourglass). Due to the good correlation between the calculation results and the tests, it can be concluded that the choice of the FE mesh size is optimal.

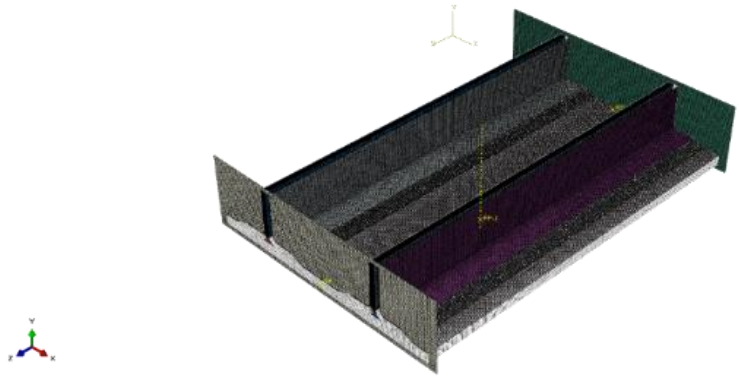

Fig. 5. Finite element model of the panel

2.2.3 Material model

One of the key factors in post-impact compression modeling is the material model, which requires a set of input properties to work correctly. For unidirectional carbon fiber reinforced plastic, this involves testing to obtain the most accurate material properties, a thorough characterization that includes separate fiber, matrix and interface tests. Both standardized and non-standardized test methods can be used to measure the elastic properties of the material, allowing to obtain the following necessary material characteristics: values of layer strength, interface and critical energy release rates in three dimensions of material direction (longitudinal, transverse and shear). Since in this mathematical model the methodology of layer-by-layer modeling was used, the compression properties of the monolayer are set as the elastic properties of the composite material (Table 3).

Table 3- Material properties

Properties	ASTM standard	Value
Elastic properties of the monolayer		
E_{1t}, GPa	ASTM D7291	159
E_{1c}, GPa	ASTM D3410	144
E_{2t}, GPa	ASTM D3039	9.095
E_{2c}, GPa	ASTM D3410	8.85
$G_{12} = G_{13}$,GPa	ASTM D3518	4.17
$\nu_{13} = \nu_{12}$	ASTM D3039	0.34
ν_{23}	ASTM D3410	0.34
Strength properties of the monolayer		
X^{T}, MPa	ASTM D7291	3255
Y^{C}, MPa	ASTM D3410	1325
Y^{T}, MPa	ASTM D3039	77
Y^{C}, MPa	ASTM D3410	232
S^{L}, MPa	ASTM D2344	103

Destruction Modes		
$g_{1+}, kJ/m^2$	Pinho et al.	150
Cross-layer properties		
τ_3^0	ASTMD7291	53.5
τ_{sh}	ASTM D2344	105
$G_{Ic,\theta=0^\circ}, kJ/m^2$	ASTM D5528	0.177

Moreover, the differentiation of load orientation is of paramount importance, since these materials exhibit different fracture properties and modes depending on whether they are subjected to tension or compression. When making non-flat joints of composite reinforced panels, such as the connection of the sheeting to the T-rib, filler is required to fill the voids between the flanges, walls and sheeting. This model uses a unidirectional carbon fiber bundle to provide local reinforcement and increase bending stiffness. Properties of the filler are presented in Table 4 [32].

Table 4. Properties of the filler

Properties	E_1, MPa	E_2, MPa	E_3, MPa	$\nu_{13}=\nu_{12}$	$G_{12}=G_{13}$,MPa	G_{23}, MPa
Value	72000	8000	8000	0.3	5000	3000

2.2.4 Model for Crack Growth and Delamination

During loading of laminated composites, the key defect is delamination, because it reduces the strength of the structure and it is very difficult to detect it without the use of special equipment. This process can be modeled using a bonded layer, for which contact stresses are set and a failure criterion is initialized. The law is then determined which damage growth occurs. With this in mind, elements are removed, allowing the process of layer separation to be visualized. The quadratic nominal stress traction-separation law" [33] used in this paper considers the interaction between the stress components and is defined as:

$$\left(\frac{\langle t_n \rangle}{t_n^0}\right)^2 + \left(\frac{t_s}{t_s^0}\right)^2 + \left(\frac{t_t}{t_t^0}\right)^2 = 1, \quad (2)$$

where t_n^0, t_s^0 and t_t^0 - peak values of nominal stress when the interface deformation occurs exclusively in the normal direction or in the first or second shear direction. The symbol $\langle\ \rangle$, used in the nominal stress designation in the normal direction is interpreted as a pure compressive stress that does not cause damage.

The law of damage evolution describes the rate at which the cohesive stiffness deteriorates after the corresponding criterion is reached. A scalar variable D, varying from 0 (no damage) to 1 (delamination), is introduced. This new variable modifies the stress components predicted by the elastic tensile/separation behavior for an undamaged material $\left(\overline{t}_n, \overline{t}_s, \overline{t}_t\right)$:

$$t_n = \begin{cases} (1-D)\,\overline{t}_n, & \overline{t}_n \geq 0 \\ \overline{t}_n \end{cases}$$
$$t_s = (1-D)\,\overline{t}_s \tag{3}$$
$$t_t = (1-D)\,\overline{t}_t$$

Damage growth with a combination of normal and shear deformation at the interface is described by the effective displacement:

$$\delta_m = \sqrt{\langle \delta_m \rangle^2 + \delta_s^2 + \delta_t^2}$$
$$G_n = \int_0^{\delta_n^f} t_n d\delta_n$$
$$G_s = \int_0^{\delta_s^f} t_s d\delta_s \tag{4}$$
$$G_t = \int_0^{\delta_t^f} t_t d\delta_t$$

Where G_n, G_s, G_t - fracture energies of the normal and two shear modes. In this case, the sum of all energies:

$$G_T = G_n + G_s + G_t \tag{5}$$

Since only two of the three previously defined relations are independent, we introduce a new value:

$$G_S = G_s + G_t \tag{6}$$

The definition of damage development is given by the energy when the criterion is fulfilled:

$$\left(\frac{G_n}{G_n^C}\right)^\alpha + \left(\frac{G_s}{G_s^C}\right)^\alpha + \left(\frac{G_t}{G_t^C}\right)^\alpha = 1, \tag{7}$$

The second component of the damage development definition is the variable D, which describes linear softening:

$$D = \frac{\delta_m^f (\delta_m^{\max} - \delta_m^0)}{\delta_m^{\max} (\delta_m^f - \delta_m^0)}, \tag{8}$$

Where δ_m^f - displacement calculated from the fracture energy G^C; δ_m^0 - displacement at the start of fracture; $\delta_m^{\max}$ - maximum value of effective displacement achieved during the loading history to simulate compression after impact, computational repetition of elementary specimen tests according to ASTM D5528 and ASTM D7905 was performed to obtain additional properties to specify the cohesive contact and to further develop delamination and fracture. The first and second modes of interlayer fracture toughness were determined from the simulation results Fig. 6 [34-35]:

$$G_{Ic} = \frac{3P\delta}{2ba}, \tag{9}$$

Where P - force, N, δ - displacement of the load application point, mm, b - specimen width, mm, a - delamination length, mm

$$G_{IIc} = \frac{3mP_{\max}^2 a_0^2}{2B}, \tag{10}$$

Where $P_{\max}$ - maximum strength, , a_0 - crack length, mm, B - specimen width, mm, m - calibration factor. Damage variable for cohesive is a dimensionless quantity that determines the presence of delamination. A value of damage variable for cohesive surfaces >1 indicates the presence of delamination.

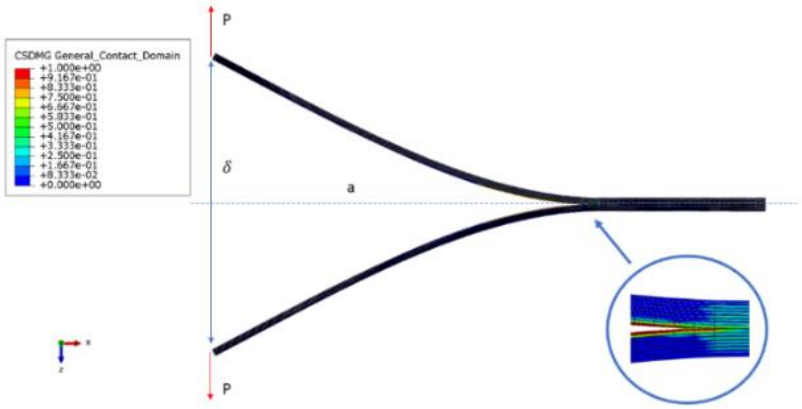

(a)

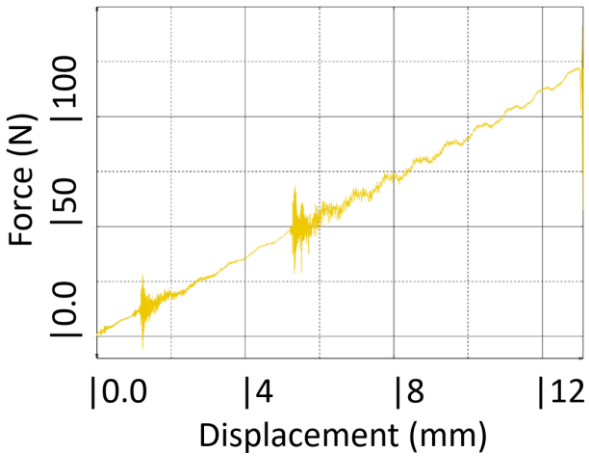

(b)

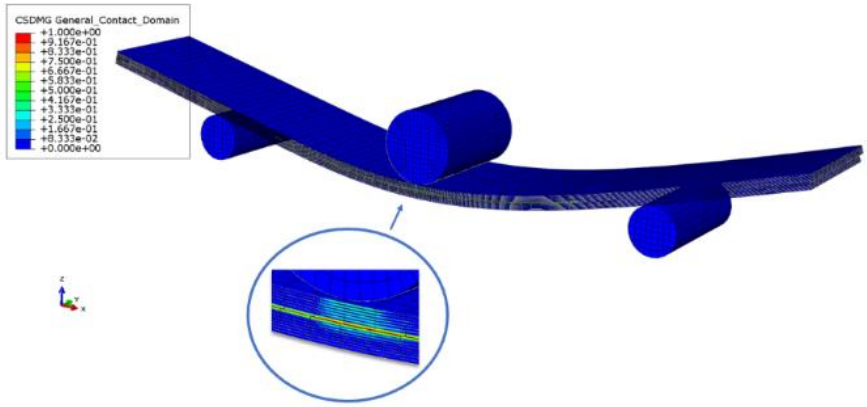

(c)

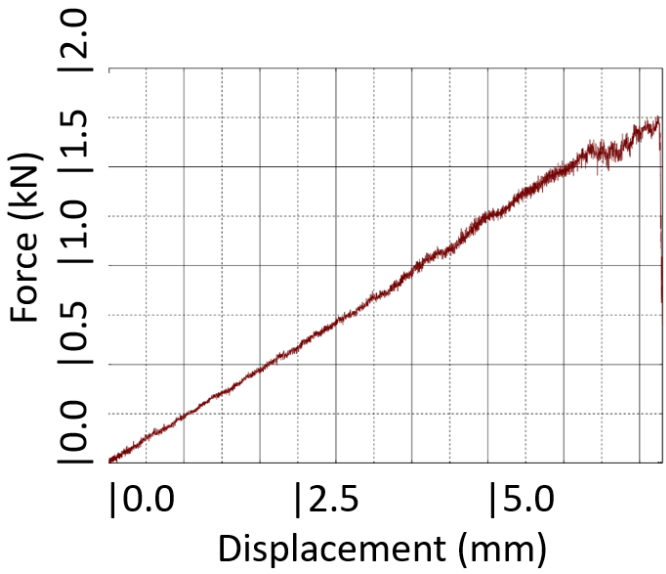

(d)

Fig. 6. (a) Damage variable for cohesive surfaces (delamination)*. General view of ASTM D5528, (b) Force (N) vs. displacement (mm) (ASTM D5528), (c) Damage variable for cohesive surfaces (delamination)*. General view of ASTM D7905 EE, (d) Force (N) vs. displacement (mm) (ASTM D7905)

3. Results and discussion

After bench tests, determination of interlayer fracture properties based on the calculation of elementary specimens, preparation of a finite-element model and additional specification of characteristics to set the material model, the following results were obtained:

- When simulating impact in the panel 10.8 mm, the defect zone was obtained in the size of 46x50 mm, in the conducted tests - 49x52 mm;
- Force in the FEM simulation was obtained as 1700 kN, in tests 1630 kN (Table 5);

- Fracture pattern corresponds to the bench tests - failure occurred along the weakened section in the impact zone.

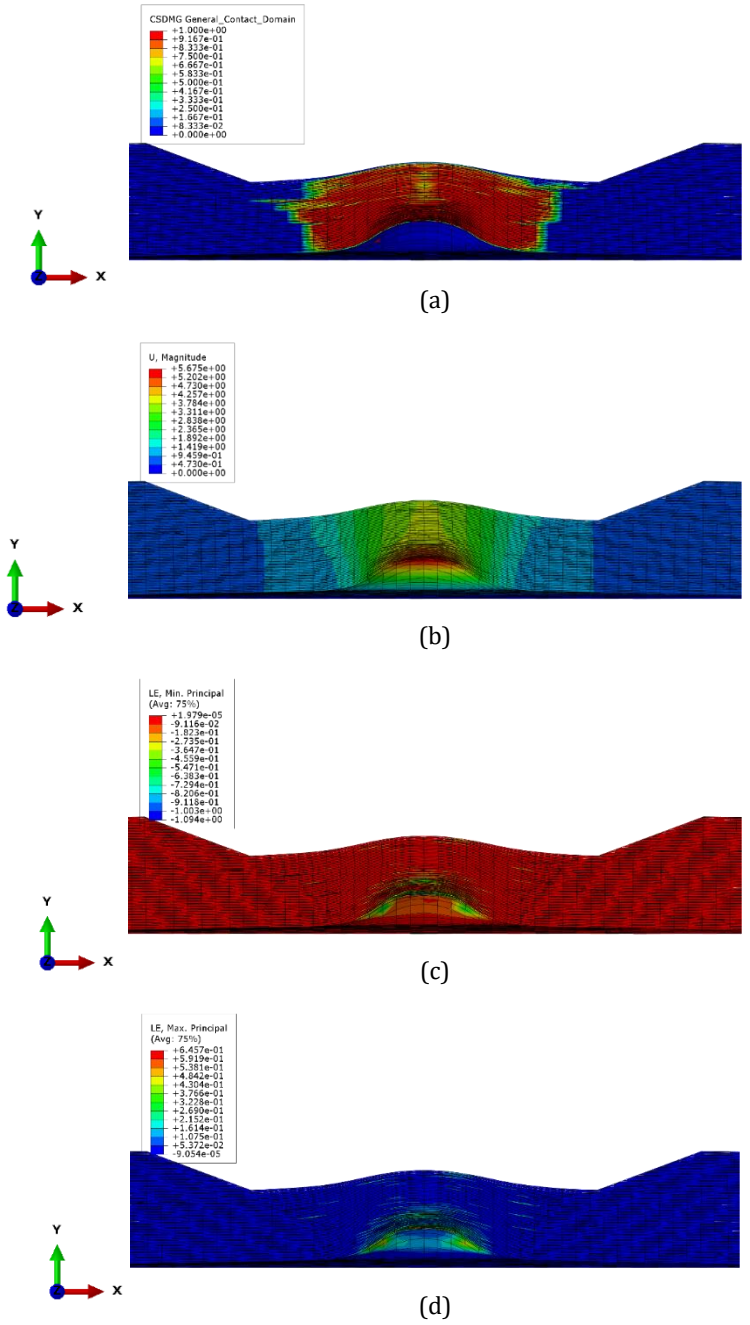

Fig. 7. (a) - Damage variable for cohesive surfaces (delamination) * after impact, (b) Total displacement in all directions (mm) in the panel after impact, (c) Maximum principal deformations (mm/mm) in the panel after impact, (d) Minimum principal deformations (mm/mm) in the panel after impact

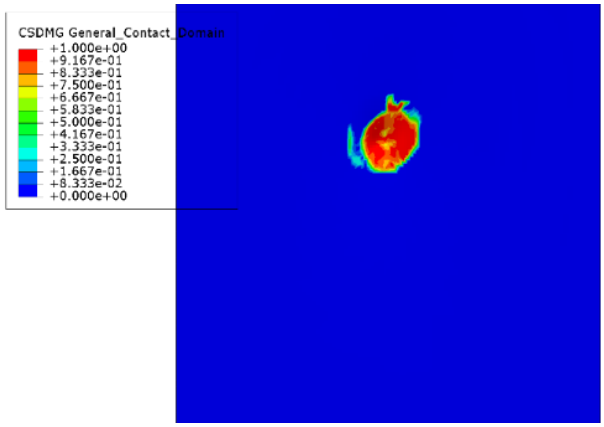

Fig. 8. 90-degree monolayer damage variable for cohesive surfaces (delamination) * (46 x 50 mm)

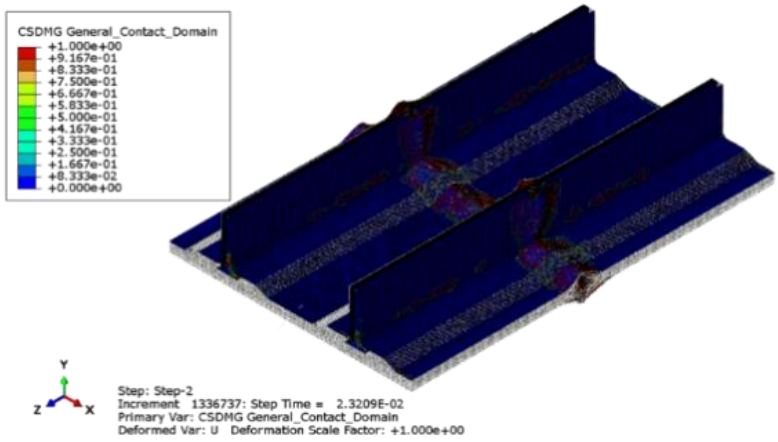

Fig. 9. Condition of the panel after fracture (Damage variable for cohesive surfaces *)

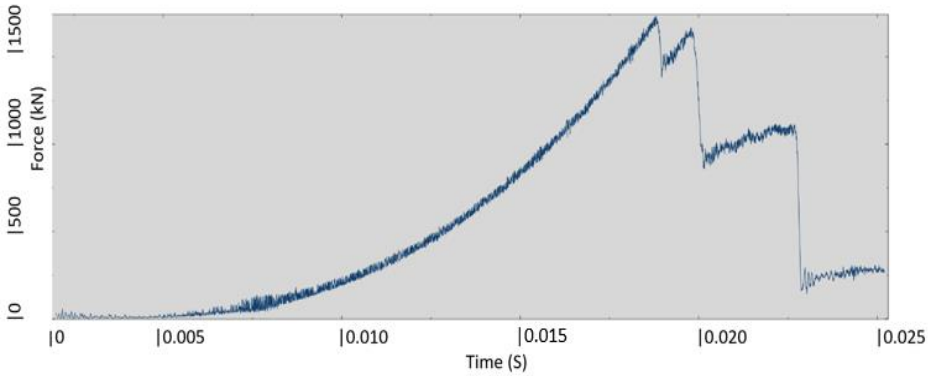

Fig. 10. Graph of the reaction force (kN) of the FEM under compression over time (s)

The discrepancy in the ultimate compression force of the damaged panel was 4.1 %. Fig 7 shows a cross-section of the panel in the XY plane after the first step of the finite-element model. The state of the panel after compression is shown in Fig. 9 and the variation of the reaction force with time obtained from FEM is presented in Fig. 10. An example of delamination in a monolayer for 90-degree direction is presented Fig. 8.

Table 5. Comparative analysis of research results

Criterion	Experiment	FEM analysis
Dimensions of the defect zone after impact damage, mm	49x52	46x50
Reaction force when determining residual compressive strength, kN	1630	1700

4. Conclusion and Future Work

The modeling methodology proposed in this paper allows for a direct comparison of not only the values of forces, stresses and deformations, but also the geometric dimensions, shape and depth of delamination between experimental samples of structures and calculation models.

The modeling technique developed and tested within the framework of the proposed study allows not only to take into account the three-dimensional stress-strain state of the structure at the monolayer level, unlike most approaches, but also allows for delamination due to detailed modeling of the contact between each layer, taking into account the compliance of the binder and the interlayer fracture toughness. Based on the calculated repetition of elementary samples according to ASTM D7905 and ASTM D5528 standards, the nature of delamination and the values of interlayer fracture toughness showed good convergence with the test results. Thus, the developed model makes it possible to obtain a representative picture of delamination for panels of great thickness, the application of which is relevant in the aerospace industry in the design of long-haul aircraft.

An acceptable qualitative similarity of the modeled fracture mechanism and form with that observed in the experiments was noted. The discrepancy in the ultimate compression force of the damaged panel was 4.1 %. The given provisions prove the possibility to use the developed technology for modeling shock damage and subsequent compression to failure of composite aircraft structures with an accuracy acceptable for engineering solutions.

In the future, the authors of this work plan to perform an assessment of the residual strength of reinforced composite panels when impact damage is applied to areas of manufacturing defects i.e. delamination, an assessment of strength recovery after impact damage repair, and an assessment of their residual strength when repeated impact damage is applied to the repair area, using the demonstrated layered modeling method to represent the adhesive repair patch and its connection to the prepared panel surface.

References

[1] Park D, Yu T, Park S, Shin D, Kim Y. Improvement of impregnation quality on out-of-autoclave processed CFRP aircraft wing spar through resin flow simulation. The Functional Composites and Structures. 2021;3:025001. https://doi.org/10.1088/2631-6331/abf480

[2] Mangalgiri P. Design allowable considerations for use of laminated composites in aircraft structures. J Indian I Sci. 2013;93(4):571.

[3] Geng J, Zhang X, Wang C. Predicting dynamic response of stiffened-plate composite structures in a wide-frequency domain based on Composite B-spline Wavelet Elements

Method (CBWEM). Int J Mech Sci. 2018;144. https://doi.org/10.1016/j.ijmecsci.2018.06.031
[4] Fedulov B, Fedorenko A, Kantor M, Lomakin E. Failure analysis of laminated composites based on degradation parameters. On-line J Meccanica. 2017; Springer:14. https://doi.org/10.1007/s11012-017-0735-9
[5] Zhang X, Chen Y, Hu J. Recent advances in the development of aerospace materials. Prog Aerosp Sci. 2018;97:34. https://doi.org/10.1016/j.paerosci.2018.01.001
[6] Barricelli B, Casiraghi E, Fogli D. A Survey on Digital Twin: Definitions, Characteristics, Applications, and Design Implications. IEEE Access. 2019;7:19143996. https://doi.org/10.1109/ACCESS.2019.2953499
[7] Alam M. Crack penetration and deflection behavior at interfaces. PhD dissertation. Oregon State University; 2016. Corvallis, OR, p. 77.
[8] Pogosyan M, Nazarov E, Bolshikh A, Korolskii V, Turbin N, Shramko K. Aircraft composite structures integrated approach: a review. J Phys Conf Ser. 2020;1925. https://doi.org/10.1088/1742-6596/1925/1/012005
[9] Easy Access Rules for Large Aeroplanes (CS-25) (Amendment 26). European Union Aviation Safety Agency; 2021.
[10] Feigenbaum YM, et al. Ensuring the strength of composite aircraft structures considering the random operational shock effects: a monograph. Moscow: TECHNOSPHERA; 2018. 506 p.
[11] Mitrofanov O, Pavelko I, Varickis S, Vagele A. An applied method for predicting the load-carrying capacity in compression of thin-wall composite structures with impact damage. Mech Compos Mater. 2018;54(1):99-110. https://doi.org/10.1007/s11029-018-9722-z
[12] Mitrofanov OV, Pavelko IV, Konstantinov VA, Esaulenko AV. Features of the methodology of designing load-bearing panels of composite materials in compression considering the damage from shock influences. Nat Techn Sci. 2018;1(115):109-112.
[13] Thorsson SI, Sringeri SP, Waas AM, Justusson BP, Rassaian M. Experimental investigation of composite laminates subject to low-velocity edge-on impact and compression after impact. Composite Structures. 2018;186:335-346. https://doi.org/10.1016/j.compstruct.2017.11.084
[14] Sachse R, Pickett AK, Middendorf P. Simulation of impact and residual strength of thick laminate composites. Compos Part B Eng. 2020;195:108070. https://doi.org/10.1016/j.compositesb.2020.108070
[15] Lopes CS, Camanho PP, Gürdal Z, Maimí P, González EV. Low-velocity impact damage on dispersed stacking sequence laminates. Part II: Numerical simulations. Compos Sci Technol. 2009;69:937-947. https://doi.org/10.1016/j.compscitech.2009.02.015
[16] Ratwani MM. Effect of damage on strength and durability. PhD thesis; 2012.
[17] ASTM International. Standard Test Method for Measuring the Damage Resistance of a Fiber-Reinforced Polymer Matrix Composite to a Drop-Weight Impact Event. ASTM D7136-14. 2014.
[18] FAA Advisory Circular AC 20-107.
[19] Pany C. An insight on the estimation of wave propagation constants in an orthogonal grid of a simple line-supported periodic plate using a finite element mathematical model. Front Mech Eng. 2022;8:926559. https://doi.org/10.3389/fmech.2022.926559
[20] Pany C, Li G. Application of periodic structure theory with finite element approach. Front Mech Eng. 2023;9:1192657. https://doi.org/10.3389/fmech.2023.1192657
[21] Sreadha AR, Pany C. Static, free vibration and buckling analysis of composite panels; a review. Adv J Graduate Res. 2021;9(1):21-45. https://doi.org/10.21467/ajgr.9.1.21-45
[22] Shah SZH, Karuppanan S, Megat-Yusoff PSM, Sajid Z. Impact resistance and damage tolerance of fiber reinforced composites: A review. Composite Structures. 2019;217:100-121. https://doi.org/10.1016/j.compstruct.2019.03.021

[23] Jefferson AJ, Srinivasan SM, Dhakal AH. Parameters influencing the impact response of fiber-reinforced polymer matrix composite materials: A critical review. Composite Structures. 2019;224:111007. https://doi.org/10.1016/j.compstruct.2019.111007
[24] Malhotra A, Guild FJ. Impact Damage to Composite Laminates: Effect of Impact Location. Appl Compos Mater. 2014;21(1). https://doi.org/10.1007/s10443-013-9382-z
[25] Kudryavtsev OA, Ignatova AV, Olivenko NA. The influence of thickness on residual flexural strength of composite with low-velocity impact damages: Experimental study. Bull Perm Natl Res Polytech Univ. Mech. 2021;3:6-11. https://doi.org/10.15593/perm.mech/2021.3.01
[26] Sergeichev IV, Anton FK, Safonov AA, Ushakov AE. Estimation of the residual strength of the elements of composite structures after a low-speed impact. J Mach Manufact Reliab. 2013;42(1):29-35. https://doi.org/10.3103/S1052618813010111
[27] Tuo H, Lu Z, Ma X, Xing J, Zhang C. Damage and failure mechanism of thin composite laminates under low-velocity impact and compression-after-impact loading conditions. Compos Part B Eng. 2019;163:642-654. https://doi.org/10.1016/j.compositesb.2019.01.006
[28] Tan W, Falzon BG, Chiu LNS, Price M. Predicting low velocity impact damage and Compression-After-Impact (CAI) behaviour of composite laminates. Compos Part B Eng. 2015;71:212-226. https://doi.org/10.1016/j.compositesa.2015.01.025
[29] Li N, Chen PH. Experimental investigation on edge impact damage and Compression-After-Impact (CAI) behavior of stiffened composite panels. Composite Structures. 2016;138:134-150. https://doi.org/10.1016/j.compstruct.2015.11.060
[30] Soto A, González EV, Maimí P, Martín de la Escalera F, Sainz de Aja JR, Alvarez E. Low velocity impact and compression after impact simulation of thin ply Laminates. Compos Part A Appl Sci Manuf. 2018;109(1):413-427. https://doi.org/10.1016/j.compositesa.2018.03.017
[31] Panettieria E, Fanteriaa D, Montemurrob M, Frousteyc C. Low-velocity impact tests on carbon/epoxy composite laminates: A benchmark study. Compos Part B Eng. 2016;107:9-21. https://doi.org/10.1016/j.compositesb.2016.09.057
[32] Hexcel. 8552 IM7 Unidirectional Prepreg 190 gsm & 35%RC Qualification Material Property Data Report. CAM-RP-2009-015 Rev B.
[33] Olivares-Ferrer JA. Finite elements modeling of Compression-After-Impact test for laminated composite thin plates with initial delaminations. Master's Thesis. Universidad de Politècnica de València, Valencia, Spain; 2018.
[34] ASTM International. Standard Test Method for Mode I Interlaminar Fracture Toughness of Unidirectional Fiber-Reinforced Polymer Matrix Composites. ASTM D5528/D5528M-21. 2021.
[35] ASTM International. Standard Test Method for Determination of the Mode II Interlaminar Fracture Toughness of Unidirectional Fiber-Reinforced Polymer Matrix Composites. ASTM D7905/D7905M-14. 2014. doi:10.1520/D7905_D7905M-14. https://doi.org/10.1520/D7905_D7905M-14